Available online at www.sciencedirect.com
ScienceDirect
European Journal of Pharmaceutics and Biopharmaceutics 70 (2008) 85–97
European Journal of Pharmaceutics and Biopharmaceutics
www.elsevier.com/locate/ejpb

Research paper

Preparation, characterization and *in vitro* cytotoxicity of indomethacin-loaded PLLA/PLGA microparticles using supercritical CO_2 technique

Yunqing Kang [a], Jiang Wu [a,b], Guangfu Yin [a,*], Zhongbing Huang [a], Yadong Yao [a], Xiaoming Liao [a], Aizheng Chen [a], Ximing Pu [a], Li Liao [a]

[a] *College of Materials Science and Engineering, Sichuan University, Chengdu, PR China*
[b] *Institute of Biomedical Engineering, West China Center of Medical Sciences, Sichuan University, Chengdu, PR China*

Received 15 December 2007; accepted in revised form 14 March 2008
Available online 29 March 2008

Abstract

In this work, indomethacin-loaded poly(L-lactic acid)/poly(lactide-co-glycolide) (IDMC-PLLA/PLGA) microparticles were prepared using solution-enhanced dispersion by supercritical fluids (SEDS) technique in an effort to obtain alternative IDMC formulation for drug delivery system. Surface morphology, particle size and particle size distribution, drug encapsulation efficiency, drug release kinetics, *in vitro* cytotoxicity and the cellular uptake of drug-loaded microparticles were investigated. The drug-loaded microparticles exhibited sphere-like shape and small particle size with narrow particle size distribution. IDMC was amorphously dispersed within the PLLA/PLGA matrix after the SEDS process. *In vitro* release studies revealed that the drug-loaded microparticles substantially enhanced the dissolution rate of IDMC compared to the free IDMC, and demonstrated a biphasic drug release profile. *In vitro* cytotoxicity assays indicated that drug-loaded microparticles possessed longer sustained inhibition activity on proliferation of the non-small-cell lung cancer A549 cell lines than did free IDMC. Fluorescence microscopy and transmission electron microscopy identified the phagocytosis of drug-loaded microparticles into the A549 cells and characteristic morphology of cell apoptosis such as the nuclear aberrations, condensation of chromatin, and swelling damage in mitochondria. These results collectively suggested that IDMC-PLLA/PLGA microparticles prepared using SEDS would have potentials in anti-tumor applications as a controlled drug release dosage form without harmful organic solvent residue.

Keywords: Supercritical CO_2; Indomethacin; Poly(L-lactic acid); Poly(lactide-co-glycolide); Microparticles; Drug delivery system

1. Introduction

Biodegradable drug carrier is becoming increasingly important for drug delivery applications [1,2]. Encapsulation of drugs within the degradable polymer microparticles can provide sustained release, reduce the side effects of drugs, and increase their bioavailability [3]. Control over particle size and particle size distribution of drug carriers is essential for good efficacy of drug delivery, as smaller particle size and narrower particle size distribution provide easier flexibility of administration. This also increases the bioavailability of the drug, leading to smaller dosages and enhancing controlled release [4]. Therefore, encapsulation of drugs has attracted a great deal of research attentions. Many techniques can be used for drug encapsulation. Yet traditional methods used for the encapsulation of drugs into polymer particles, such as spray drying, emulsification/solvent evaporation method and its modified versions, are beset with some problems [5]. Some of these techniques generally provide limited control over the particle size and particle size distribution. Furthermore, to

* Corresponding author. College of Materials Science and Engineering, Sichuan University, Wangjiang Road 29#, Chengdu, Sichuan 610064, PR China. Tel./fax: +86 28 8541 3003.
E-mail address: nic0700@scu.edu.cn (G. Yin).

0939-6411/$ - see front matter © 2008 Elsevier B.V. All rights reserved.
doi:10.1016/j.ejpb.2008.03.011

reduce the residual organic solvent to low level, many downstream processes such as additional drying step have to be performed [6,7].

The use of supercritical fluid (SCF) techniques has provided a 'clean' and effective alternative to traditional methods of drug and polymer processing, while circumventing many of the problems associated with traditional techniques [8]. Supercritical CO_2 ($scCO_2$), which is by far the most widely used SCF in drug delivery applications, is relatively inexpensive, non-toxic and non-flammable [9]. Solution-enhanced dispersion by supercritical fluids (SEDS) technique was developed by the Bradford University in order to achieve smaller droplet size and intense mixing of supercritical fluid and solution for increased transfer rates [10,11]. SEDS is a modified supercritical anti-solvent (SAS) process, in which SCF and the liquid polymer solution are together sprayed into a high pressure vessel using a specially designed coaxial nozzle. The SCF is used as both anti-solvent for its chemical properties and 'spray enhancer' by mechanical effect. The spontaneous contact of high-speed streams of SCF and a liquid solution generates the finely dispersed mixture and a prompt particle precipitation [12,13]. Several researchers had successfully synthesized drug-loaded polymer microparticles or significantly reduced the particle size of the drugs using SCF-based technologies. For example, Chattopadhyay and Gupta [14] produced antibiotic nanoparticles using $scCO_2$ anti-solvent methods. Elvassore et al. [15] reported that protein-loaded poly(lactic acid) could be prepared by adding a $scCO_2$ anti-solvent to an organic solvent solution of protein and polymer. The group of Johnston at the University of Texas had reported a number of novel supercritical processes, such as spray freezing into liquid, for enhancing the dissolution of poorly water-soluble drugs and for encapsulating drugs [16–18]. In our previous study [19], we had succeeded in using SCF technique to micronize 5-Fluorouracil and to load 5-Fluorouracil into PLLA microparticles. However, few researchers reported that indomethacin was encapsulated into PLLA/PLGA polymers microparticles by the SEDS process.

Indomethacin (IDMC), a non-steroidal anti-inflammatory drug (NSAID) with analgesic and anti-pyretic properties [20,21], has been widely used to reduce the inflammation and pain in patients suffering from arthritis. Interestingly, substantial experimental and clinical evidences have indicated a role of NSAIDs in the prevention of various types of cancer [22,23], especially when combined with chemotherapy [24–26]. Epidemiological studies have also shown that regular use of NSAID reduces the risk of developing cancers [26,27]. NSAIDs, including IDMC, can inhibit cell proliferation and induce apoptosis in a number of cancer cell lines *in vitro*, which is considered to be an important mechanism for their anti-tumor activity and prevention of carcinogenesis. However, their efficacies are offset by significant incidence of gastrointestinal ulceration and haemorrhage. IDMC also inhibits gastric mucosal secretion, active bicarbonate secretion from gastric mucosa, and reduces mucosal blood flow. Furthermore, IDMC is generally a highly crystalline and poorly water-soluble drug [28,29]. Many attempts have been made to reduce the side effects associated with IDMC by delivering microparticles containing low dosage of drug directly to intended site, and to improve its solubility by stabilizing the amorphous form of the drug within a polymeric matrix, as amorphous pharmaceuticals have their potential to enhance the bioavailability of drugs [30].

Poly(L-lactide) (PLLA) and poly(lactide-co-glycolide) (PLGA) have been widely studied as a matrix material for drug delivery systems due to their biodegradability and biocompatibility [31–33]. In our previous study [19], PLLA microparticles with the mean particle size of 1.86 μm were successfully prepared by the SEDS process. But we also found that it was more difficult to form fine particles from amorphous PLGA polymers alone than from semi-crystalline PLLA polymers by the SEDS process, as reported in the literature [34]. Semi-crystalline PLLA and amorphous PLGA have different nucleation rates in the supercritical process [13]. Therefore, in this work, a new biodegradable polymer matrix (the blends of PLLA and PLGA) was prepared by the SEDS process, thus not only solving the particle formation problem of PLGA but also modulating the degradation rate of PLLA/PLGA blends due to the different degradation rate of PLLA and PLGA [35–37]. The laser particle size analyzer was applied to measure the mean particle size and particle size distribution of the obtained microparticles, and scanning electron microscopy (SEM) was employed to study surface morphology. The drug loading, encapsulation efficiency, and *in vitro* drug release kinetics were measured by ultraviolet absorption. The change in crystallinity of drug-loaded microparticles after the SEDS process was investigated by X-ray diffraction (XRD). Thermal behavior of IDMC-loaded microparticles was investigated via differential scanning calorimeter (DSC). The interaction of IDMC and PLLA/PLGA matrix after encapsulation was then studied by Fourier transform infrared (FTIR). *In vitro* therapeutic effect of the IDMC-loaded microparticles was investigated by assaying the cell viability of non-small-cell lung cancer A549 cell lines, which was conducted in comparison with that of the placebo PLLA/PLGA microparticles and that of free IDMC. *In vitro* cellular internalization of fluorescent PLLA/PLGA and IDMC-loaded PLLA/PLGA microparticles was visualized by fluorescent microscopy (FM). Phagocytosis of microparticles into the A549 cells and characteristic morphology of cell apoptosis were further identified by the observation of cell ultrathin sections under transmission electron microscopy (TEM).

2. Materials and methods

2.1. Materials

Poly(L-lactic acid) (PLLA, $M_w = 100$ kDa), poly(lactide-co-glycolide) (PLGA 50:50, $M_w = 100$ kDa) were pur-

chased from the Institute of Medical Instrument (Shandong, China). IDMC was supplied by HaiRong Pharmaceutical Co. Ltd. (Chengdu, China). CO_2 with the purity of 99.9% was supplied by Chengdu Tuozhan gas Co. Ltd. (Chengdu, China). Dichloromethane (DCM) and all other compounds were of analytical purity.

2.2. SEDS process

The diagram of the SEDS process for the preparation of microparticles is shown in Fig. 1. Experimental equipments consist of three major components: a CO_2 supply system, an organic solution delivery system, and a high pressure vessel. In order to ensure the liquefaction of the CO_2 gas and also to prevent cavitations, CO_2 fed from a CO_2 cylinder was cooled down to around 0 °C by a cooler (Maneurop, France). Then liquefied CO_2 was delivered by a high pressure meter pump to the high pressure vessel with a volume of 500 ml. The liquefied CO_2 was pre-heated to desired operating temperature by using a heat exchanger. The high pressure vessel was incubated in a gas bath to keep the temperature constant during the experiment. When the desired pressure of the high pressure vessel was reached, a steady flow (18 l/h) of $scCO_2$ was maintained by adjusting a downstream valve. When the desired pressure and temperature were stabilized (P was 12 MPa and T was 33 °C in this work), the polymer solution was delivered into the high pressure vessel through a stainless steel coaxial nozzle (ID 800 μm, and the nozzle of polymer solution with ID 330 μm was used in this study) by using a HPLC pump at the flow rate of 0.5 ml/min. When the delivery was finished, fresh $scCO_2$ was used continually to wash the products to remove the residual organic solvent for about 30 min. During the process of washing, the system operating conditions (P, T and the flow rate of $scCO_2$) were maintained as described before. After washing, the high pressure vessel was slowly depressurized and the products were collected from the side wall and the bottom of the vessel.

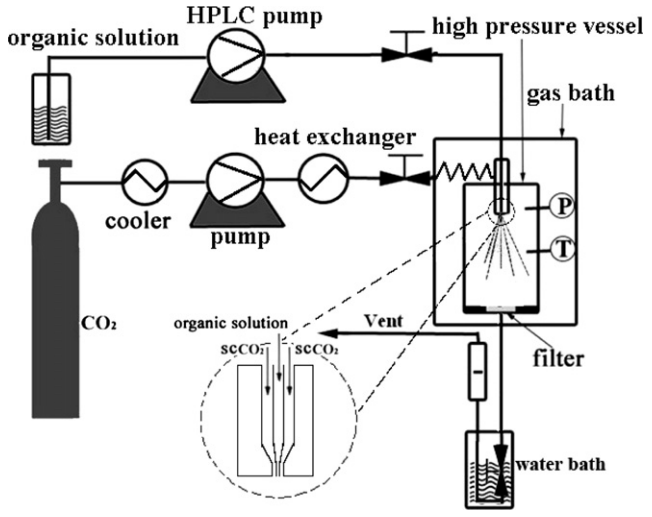

Fig. 1. Apparatus schematic diagram of the apparatus for the SEDS precipitation process.

2.3. Preparation of IDMC-PLLA/PLGA microparticles

IDMC with four times the total mass of PLLA and PLGA (i.e., the ratio of drug to polymer was 1:4, the mass ratio of PLLA to PLGA was 1:1) was together dissolved in DCM solvent and mixed completely, and the final solution concentration of PLLA/PLGA was 0.5% (w/v). The operating conditions were as described above (P: 12 MPa, T: 33 °C, the flow rates of $scCO_2$ and polymer solution were 18 l/h and 0.5 ml/min, respectively). The placebo PLLA/PLGA (1:1) microparticles were also prepared by the same SEDS process without IDMC.

To observe the cellular uptake of microparticles and morphological characteristics of cell damage under fluorescence microscope, fluorescent placebo microparticles and drug-loaded microparticles were also prepared by adding 0.5% of fluorescein into the PLLA + PLGA organic solution or IDMC + PLLA + PLGA solution, and fluorescent PLLA/PLGA or IDMC-PLLA/PLGA microparticles were obtained in the SEDS process as described above.

2.4. Characterizations

2.4.1. Particle size and particle size distribution

The mean particle size of microparticles was determined using a laser particle size analyzer (Rise-2008, Jinan Ruizhi technology Co. Ltd., Shandong). Approximately 5 mg of microparticles was dispersed in the sample cell filled with distilled water. The software of this analyzer was performed to characterize the particle size. The particle size distribution was expressed by the SPAN value (according to *the Pharmacopeias of the People's Republic of China* (2000) and [38]), which was calculated using the following equation: $\mathrm{SPAN} = (D_{90} - D_{10})/D_{50}$, where D_{10}, D_{50} and D_{90} were the diameters at 10%, 50% and 90% cumulative volumes, respectively.

2.4.2. Surface morphology

The surface morphology of IDMC-PLLA/PLGA microparticles and PLLA/PLGA microparticles was observed using a scanning electron microscope (JSM-5900LV, Japan). Before the observation, microparticles samples were stuck on a standard stand using a double-sided sticky tape.

2.4.3. XRD and FTIR

Powder X-ray diffraction (XRD) was carried out using a Philips X'Pert MDP diffractometer. The measurement was performed in the range of 10°–40° with a step size of 0.02° in 2θ using Cu Kα radiation as the source. Fourier transform Infrared (FTIR) was performed using a NEXUS spectrometer 670 (Thermo Nicolet, USA). Approximately 1 mg of microparticles was ground with KBr and pressed into a thin tablet.

2.4.4. DSC thermal analysis

Differential scanning calorimetry (DSC, 200PC, NETZSCH, Germany) was used to measure the effects of the SEDS process on the glass transition behaviors (T_g) of polymer samples and examine the dispersion formation of drugs in polymeric microparticles matrix. Approximately 5 mg of microparticles was loaded in the aluminum pans, and then the pans were sealed and heated under nitrogen atmosphere (investigated temperature range: 0–300 °C, heating rate: 5 °C/min).

2.4.5. Determination of drug loading (DL) and encapsulation efficiency (EE)

Accurately weighed 50 mg sample of IDMC-PLLA/PLGA microparticles was suspended in 10 ml of ethanol and stirred for 10 s to wash the loosely attached IDMC on the surface of microparticles or the unencapsulated free IDMC, and then the centrifuge tubes were centrifuged at 4000 rpm for 15 min. After removing the supernatant liquid, the precipitated microparticles were dissolved in 5 ml of DCM, and then 20 ml of 0.4% NaOH solution was added and stirred by a magnetic force stirrer to volatilize the DCM. The resulting solution was filtrated through a 0.22-μm membrane filter, and the amount of IDMC in the filtered solution was analyzed by UV spectrophotometer (U3010, Hitachi, Japan) at 320 nm, according to the standard curve of IDMC. The drug loading and encapsulation efficiency were calculated by Eqs. (1) and (2), respectively. Each experiment was carried out in independent triplicate.

$$\mathrm{DL} = \frac{\text{the mass of IDMC encapsulated in the microparticles}}{\text{the total mass of microparticles}} \times 100\% \quad (1)$$

$$\mathrm{EE} = \frac{\text{the mass of IDMC encapsulated in the microparticles}}{\text{the total mass of IDMC used in the process}} \times 100\% \quad (2)$$

2.5. In vitro release study

Twenty microgram sample of IDMC-PLLA/PLGA microparticles was put into the pretreated dialysis bag (Stone container corporation, North Chicago, USA), and the dialysis bag was hung in the middle of 150 ml ground bottle with 100 ml phosphate buffered saline (PBS, pH 6.8), then incubated in a water-bath shaker at 37 °C at 60 rpm. Ten milliliter of solution was periodically removed and the concentration of IDMC was analyzed by UV spectrophotometer at 320 nm. In order to maintain the original PBS volume of 100 ml, 10 ml of fresh PBS was periodically added. Release profiles were calculated in terms of cumulative release percentage of IDMC (%, w/w) with incubation time. Each experiment was carried out in triplicate. Morphology change of the IDMC-PLLA/PLGA microparticles after the *in vitro* release experiment was observed by SEM.

2.6. Cell culture

Human non-small-cell lung cancer A549 cell line was obtained from American Type Culture Collection (ATCC), Maryland, USA. A549 cells were cultured in RPMI-1640 medium (Gibco Life Technologies) enriched with 10% heat-inactivated fetal calf serum (Gibco Life Technologies) and 1% penicillin/streptomycin (Gibco Life Technologies), and incubated under standardized conditions (37 °C, 5% carbon dioxide, 100% humidity).

2.7. In vitro cytotoxicity studies

The cell viability was chosen as a cytotoxicity parameter and determined by the 3-(4,5-dimethylthiazol-2-yl)-2,5-diphenyltetrazolium bromide (MTT) assay. MTT assay was applied to evaluate the effect of IDMC-PLLA/PLGA microparticles on A549 cell viability by measuring the uptake and reduction of tetrazolium salt to an insoluble formazan dye by cellular microsomal enzymes. Two hundred microliter of A549 cell suspensions (1×10^4 cells) was dispensed (three wells for each particle type) into 96-well plates (Helena BioSciences, UK) and incubated overnight (16 h) to allow for cell attachment. Culture medium was replaced with 200 μl of microparticles/culture medium suspensions in triplicate and incubated at 37 °C for 12, 24, 48 and 72 h, respectively. Microparticles/culture medium investigated in this study included three types: placebo PLLA/PLGA, free IDMC and IDMC-PLLA/PLGA group. IDMC-PLLA/PLGA microparticles/culture medium suspensions contained the same drug concentrations as free IDMC (100 μM). A549 cells without microparticles were used as the control. Next, 100 μl of MTT (1 mg/ml) solution was added into each well and was allowed to incubate at 37 °C for 4 h, and then the solution was removed and 150 μl of dimethylsulfoxide (DMSO) was added into each well. Finally the plate was incubated for 30 min at room temperature. Absorption at 490 nm was measured with Microplate Reader 3550 (Bio-Rad, USA). The cell viability was calculated by the following formula: cell viability (%) = optical density (OD) of the treated cells/OD of the non-treated cells.

To determine the IC_{50} value (the drug concentration required to inhibit growth by 50% relative to controls) of free IDMC and IDMC-PLLA/PLGA, 200 μl of A549 cell suspensions (1×10^4) was dispensed into 96-well plates and incubated overnight (16 h) to allow for cell attachment. Culture medium was replaced with 200 μl of microparticles/culture medium suspensions in triplicate at four different concentrations (25, 50, 100 and 200 μM) and incubated at 37 °C for 48 h, respectively. IC_{50} was calculated by the curve fitting of the cell viability data.

2.8. Fluorescence microscope observation of microparticles

To give direct evidence that drug-microparticles had been phagocytosized into the cells, the cellular uptake of

microparticles and inspection of apoptotic cell morphology were studied using fluorescence microscope. A549 cells were grown on coverslips for 24 h in a six-well tissue culture plate at 37 °C. The cells were then incubated with free IDMC, the fluorescent placebo microparticles and drug-loaded microparticles at a concentration of 200 μM employed in this experiment for 24 h. After washing three times with PBS (0.01 M, pH 7.2), the cells were fixed by 4% polyoxymethylene at 4 °C for 30 min, and then 0.1% Triton X-100 was added into the wells and washed by PBS after 10 min. After fixation and permeabilization, the cells were stained with BODIPY FL phallacidin (B-607, Modecular probes Inc., USA) to label the filamentous actin (F-actin) and finally counterstained with DAPI (4′,6-diamidino-2-phenylindole, dihydrochloride) (D-1306, Modecular probes Inc., USA) to label the nucleus. Then, the cells were incubated for 1 h at 37 °C and washed by PBS. The stained coverslips were mounted on a glass slide and photographed using fluorescence microscope (TE2000-S, Nikon, Japan).

2.9. Transmission electron microscopy (TEM) of microparticles in A549 cell

Sample preparation for transmission electron microscopy was done by a following typical procedure. Two hundred microliter of A549 cell suspensions (1×10^6) was dispensed into 6-well plates and incubated for 4 h. Then culture medium was replaced with 200 μl of microparticles/culture medium suspensions in triplicate and the cells were incubated with microparticles at a concentration of 200 μM for 24 h. After 24 h, the A549 cells (about 1×10^7) were washed with PBS three times and harvested by 0.25% trypsinization. The cells were centrifuged at 1500 rpm for 10 min and then the supernatant liquid was removed. About 0.5% glutaraldehyde solution at 4 °C was slowly added into the centrifuge tube through the wall of tube to fix for 30 min. Then, the cells were centrifuged at 10,000 rpm for 10 min and then the supernatant liquid was removed. The pellets of cells were further fixed by 3% glutaraldehyde solution. Fixed cells were washed with PBS and dehydrated sequentially in a graded series of acetone solutions (30%, 50%, 70%, 90% and 100%). The specimens were further embedded in resin. Ultrathin sections (approximately 50 nm in thickness) were cut with a diamond knife using an ultramicrotome (MT-X; RMC Inc., Tucson, USA). The ultrathin sections were mounted on copper grids, and stained with 2% uranyl acetate and Reynolds' lead citrate each for 7 min. The ultrastructures of A549 cell were observed with a transmission electron microscope (H-600; Hitachi, Tokyo, Japan).

2.10. Statistical analysis

All data were arranged as mean ± standard deviation. Significant differences were determined by *t*-test. $P < 0.05$ was considered to be significant.

3. Results and discussion

3.1. Morphology observation of microparticles

Fig. 2 shows the SEM of PLLA/PLGA and IDMC-PLLA/PLGA microparticles, respectively. The placebo PLLA/PLGA microparticles exhibit rather spherical shape and smooth surface (Fig. 2a). The surface morphology appears to have no significant differences between placebo microparticles and drug-loaded microparticles (Fig. 2a and b). Fig. 3 shows the particle size and particle size distribution of placebo microparticles (Fig. 3a) and drug-loaded microparticles (Fig. 3b). Two types of both microparticles indicate small particle size and narrow particle size distribution. The mean particle size of placebo PLLA/PLGA microparticles is 1.65 μm (SPAN: 0.831) and that of IDMC-PLLA/PLGA microparticles is 2.35 μm (SPAN: 0.914). The particle size of drug-loaded microparticles is slightly larger than that of placebo microparticles.

3.2. XRD of IDMC-PLLA/PLGA microparticles

Fig. 4 shows the powder X-ray diffraction patterns of free IDMC (line a), physical mixtures of IDMC and

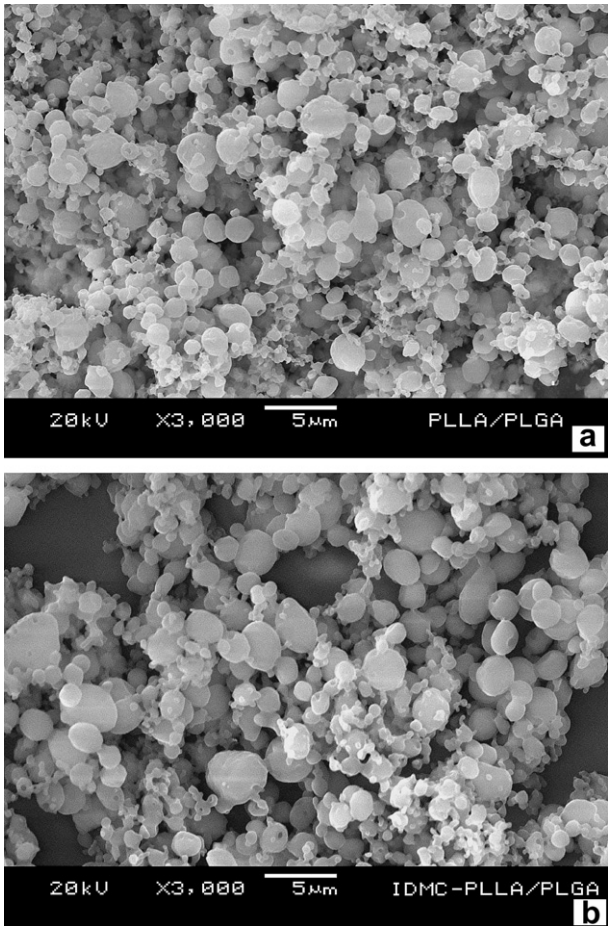

Fig. 2. SEM images of PLLA/PLGA (a) and IDMC-PLLA/PLGA microparticles (b).

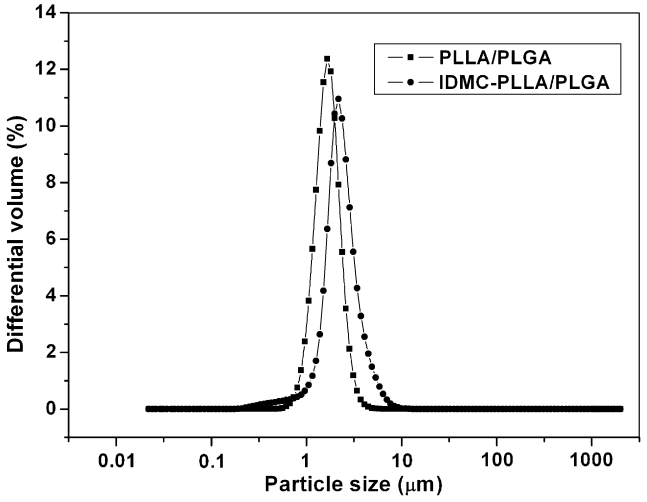

Fig. 3. The particle size and particle size distribution of placebo PLLA/PLGA (a) and IDMC-PLLA/PLGA microparticles (b). The cumulative and differential PSD are presented on the logarithmic scale.

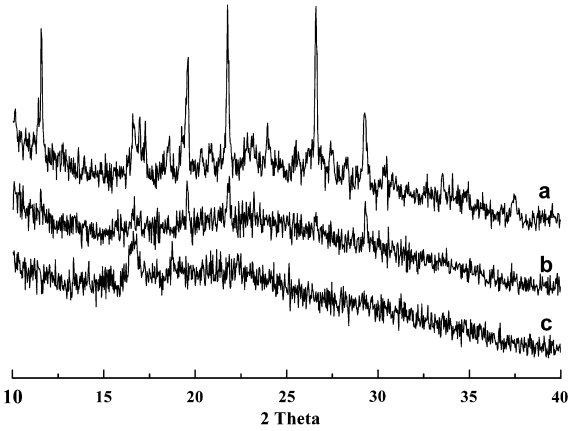

Fig. 4. XRD patterns of free IDMC (a), physical mixtures of IDMC and PLLA/PLGA (b), and IDMC-PLLA/PLGA prepared by the SEDS process (c).

PLLA/PLGA (the fraction of IDMC was similar to the content in the drug-loaded microparticles according to DL) (line b), and the IDMC-PLLA/PLGA prepared by the SEDS process (line c), respectively. In the physical mixtures, the weak characteristic peaks of crystalline IDMC can still be observed in the XRD patterns. However, for IDMC-PLLA/PLGA prepared by the SEDS process, the characteristic peaks of crystalline IDMC are very weak (line c). XRD patterns clearly show a significant decrease in crystallinity of the drug in the resultant products after processing in $scCO_2$, suggesting that the drug is dispersed in an amorphous state into the PLLA/PLGA matrix. Amorphous IDMC drug was easy to be released from the polymer matrix.

3.3. DSC analysis

The DSC analysis of the free IDMC, IDMC-loaded microparticles in the SEDS process and physical mixtures of microparticles (IDMC and PLLA/PLGA) was used to further determine whether IDMC was amorphously dispersed in the polymer matrix, and also to examine the structure changes of polymers. As shown in Fig. 5, the melting peak of crystalline IDMC is located at 162.3 °C, which is in agreement with the literature [39]. In the physical mixtures, the melting point of IDMC can be observed (Fig. 5c), indicating that crystalline IDMC can be detected. However, for IDMC-PLLA/PLGA microparticles, the intensity of melting peak of IDMC decreases dramatically (Fig. 5b), and only a small terrace can be observed at approximately 160.3 °C (inserted magnification curves). This suggests that crystalline IDMC had essentially disappeared, and a bulk of IDMC encapsulated into polymeric matrix is in an amorphous form.

It can be seen from the figures that the addition of IDMC slightly affected the glass transition temperature (T_g) and melting point (T_m) of polymers. In physical mixture, the T_g of PLGA and PLLA is at 47.7 and 60.9 °C, respectively. However, the T_g for PLGA and PLLA in IMDC-PLLA/PLGA prepared by the SEDS process is approximately 2.5 °C lower than that of physical mixture (inserted magnification curves). It is also observed that, for IDMC-loaded microparticles, the melting point of PLLA is further shifted to high temperature by approximately 6 °C (from 149.7 to 155.7 °C), suggesting there were some effects of IDMC. This might result from that amorphous IDMC was in part molecularly interacting with the amorphous region of PLLA due to the affinity between IDMC and PLLA, making it possible that crystalline regions of PLLA were more oriented and closely packed compared to the placebo PLLA/PLGA without the additive of IDMC in the SEDS process, thus leading to the slight increase of T_m of PLLA (from 149.7 to 155.7 °C).

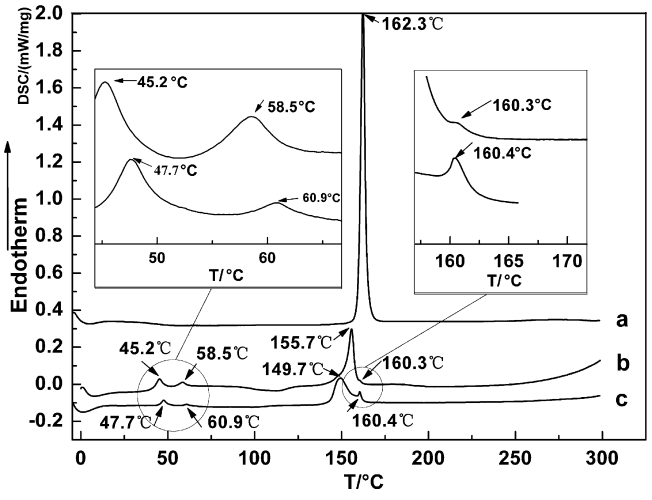

Fig. 5. DSC for free crystalline indomethacin (a), IDMC-PLLA/PLGA microparticles prepared by the SEDS process (b), and IDMC and PLLA/PLGA prepared in physical mixture (c).

3.4. FTIR characterization

Fig. 6 shows characteristic absorption peak at 1758.39 cm^{-1} for the C═O stretching in PLLA or PLGA (line a) of placebo PLLA/PLGA. Two main characteristic absorption peaks of C═O stretching (line b) are observed for crystalline IDMC at 1717.37 and 1692.03 cm^{-1}, and an absorption peak at 752.62 cm^{-1} for the C–Cl stretching [39–41]. After SEDS process (line c), the two main peaks (1717.02 and 1691.87 cm^{-1}) appear at the same position compared with the physical mixtures (line b), which indicates that there exists IDMC in the resulting products. The presence of the peak at 750.33 cm^{-1} for C–Cl stretching further confirms the successful encapsulation of IDMC in the PLLA/PLGA blend matrix.

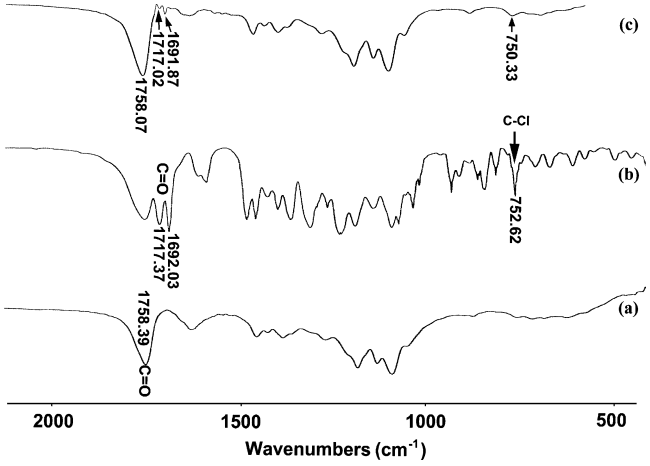

Fig. 6. FTIR of PLLA/PLGA microparticles (a), physical mixture of IDMC and PLLA/PLGA (b), and IDMC-PLLA/PLGA prepared by the SEDS process (c).

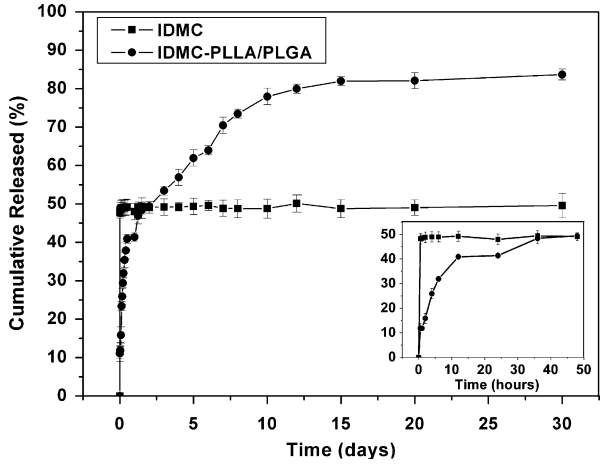

Fig. 7. *In vitro* release property of IDMC from drug-loaded PLLA/PLGA microparticles. Each point represents the mean ± standard deviation obtained from triplicates of the samples.

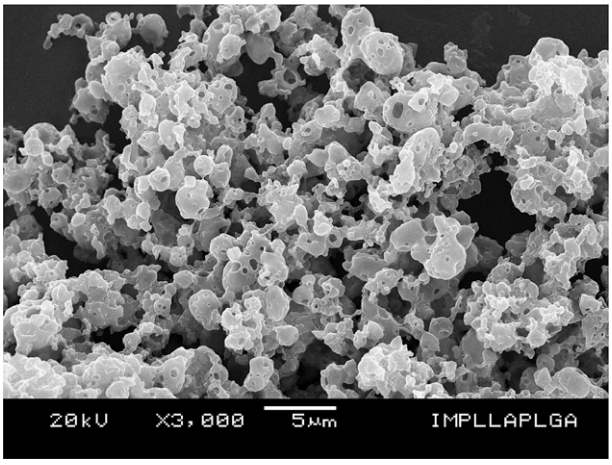

Fig. 8. SEM of IDMC-PLLA/PLGA removed out from the release medium after 30 days.

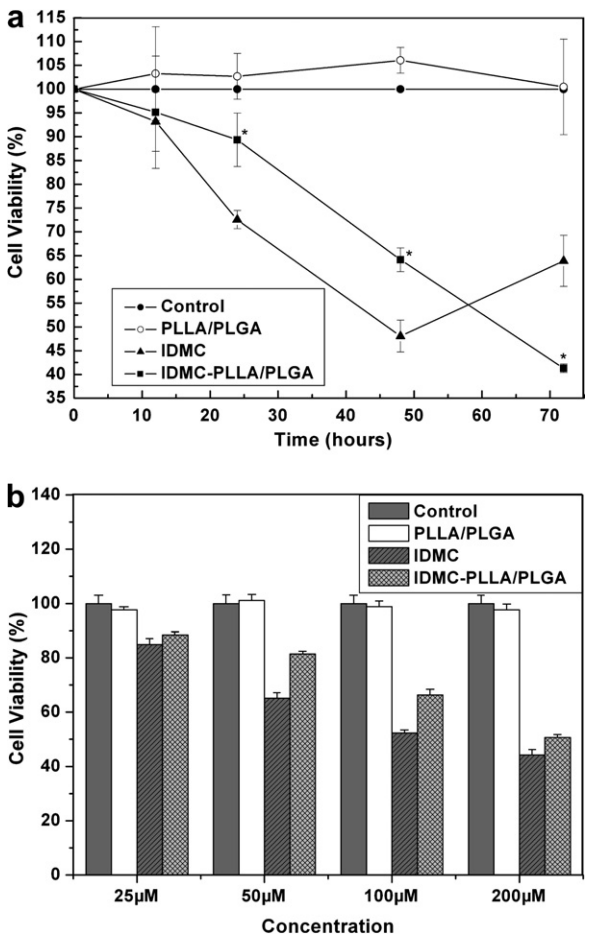

Fig. 9. (a) Cell viability of A549 cells indicating effect of the treatment time when incubated with free IDMC and IDMC-PLLA/PLGA for 12, 24, 48 and 72 h at 37 °C. IDMC-loaded PLLA/PLGA has significant sustained cell inhibition abilities in comparison with the free IDMC ($p < 0.05$). Sign ∗ represents significant difference. (b) Cell viability of A549 cells incubated with free IDMC and IDMC-PLLA/PLGA at 25, 50, 100 and 200 μM drug concentrations at 37 °C for 48 h. Error bars indicate standard deviation. Cell viability was determined by the MTT assay and expressed as a percentage of the control wells (cells without treatment).

3.5. DL and EE

DL and EE are important parameters to evaluate the properties of drug-loaded microparticles. In this study, the feeding weight ratio of drug to polymer was taken as 1:4 (i.e., theoretical drug loading of 20%). The results show that about 2.8% of the drug loading is obtained, and the EE is 14%, which is near to the drug loading of PLA microparticles prepared by CO_2-based microencapsulation technique reported by Liu [42]. It could be supposed that the low encapsulation efficiency is due to the different precipitation kinetics of the drug and polymer in the SEDS process [13]. The formation of PLLA/PLGA microparticles might be faster than that of IDMC in the SEDS process, so that the subsequent precipitated IDMC was easy to attach on the surface of firstly precipitated PLLA/PLGA microparticles. Actually, the real reason requires further studies. Obviously, it is necessary that more attempts should be made to optimize the SEDS encapsulation process to increase EE. Of course, increasing the feeding weight ratio of drug to polymer, the DL and EE might be increased. At present, this obtained result is quite promising at this feeding ratio. If significant improvements of DL and EE are obtained through the optimization of parameters of SEDS process, it would be more commercially attractive.

3.6. In vitro release study of IDMC

In vitro release property of IDMC from drug-loaded microparticles is shown in Fig. 7. It can be seen that IDMC-loaded microparticles exhibit the biphasic drug release kinetics with an initial release up to 11.85% at 0.5 h, followed by accumulative release of 83.67% after 30 days. The inset is a magnification of the release curve on the first day. It can be seen that the free IDMC rapidly reaches the saturation plateau (48.95%) in 4 h, while IDMC-PLLA/PLGA exhibits a low initial burst release (11.85% at 0.5 h) and accumulative release did not exceed that of free IDMC until after 48 h. After processing in $scCO_2$, the IDMC solubility was increased dramatically compared with free crystalline IDMC. The reason might be that crystallinity of IDMC remarkably decreased and IDMC was dispersed within polymer matrix in an amorphous form after the SEDS process. The sustained release of IDMC resulted from the diffusion of drug at the early stage and the degradation of polymers later. The degradation rate of polymer matrix depended on the ratio of PLGA to PLLA. It is well known that amorphous PLGA demonstrates rapid degradation rate compared to the semi-crystalline PLLA [36]. Therefore, the release rate of drug from the polymer matrix can be controlled by proportion of PLLA and PLGA, which is an important significance of controlling the release of drug. Of course, crystallinity and molecular weight of polymer, and particle size of microparticle also have effects on the degradation of polymer and release rate of drug. Changes in morphology of the drug-loaded PLLA/PLGA microparticles after 30 days of *in vitro* release are shown in Fig. 8. The microparticles show loss of their spherical shape and pore holes are observed. Through the degradation of polymer matrix, the drug was gradually released.

3.7. Cytotoxicity

In this study, non-small-cell lung cancer A549 cell line was used to determine the anti-tumor activity of IDMC.

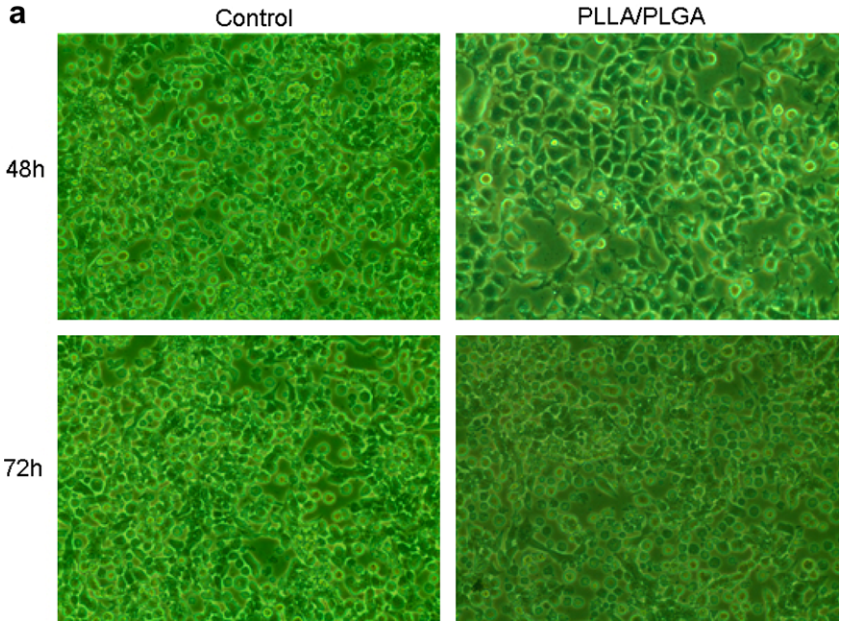

Fig. 10. The optical images of cell of control and PLLA/PLGA group (a), and IDMC and IDMC-loaded PLLA/PLGA (b) at different incubation time with A549.

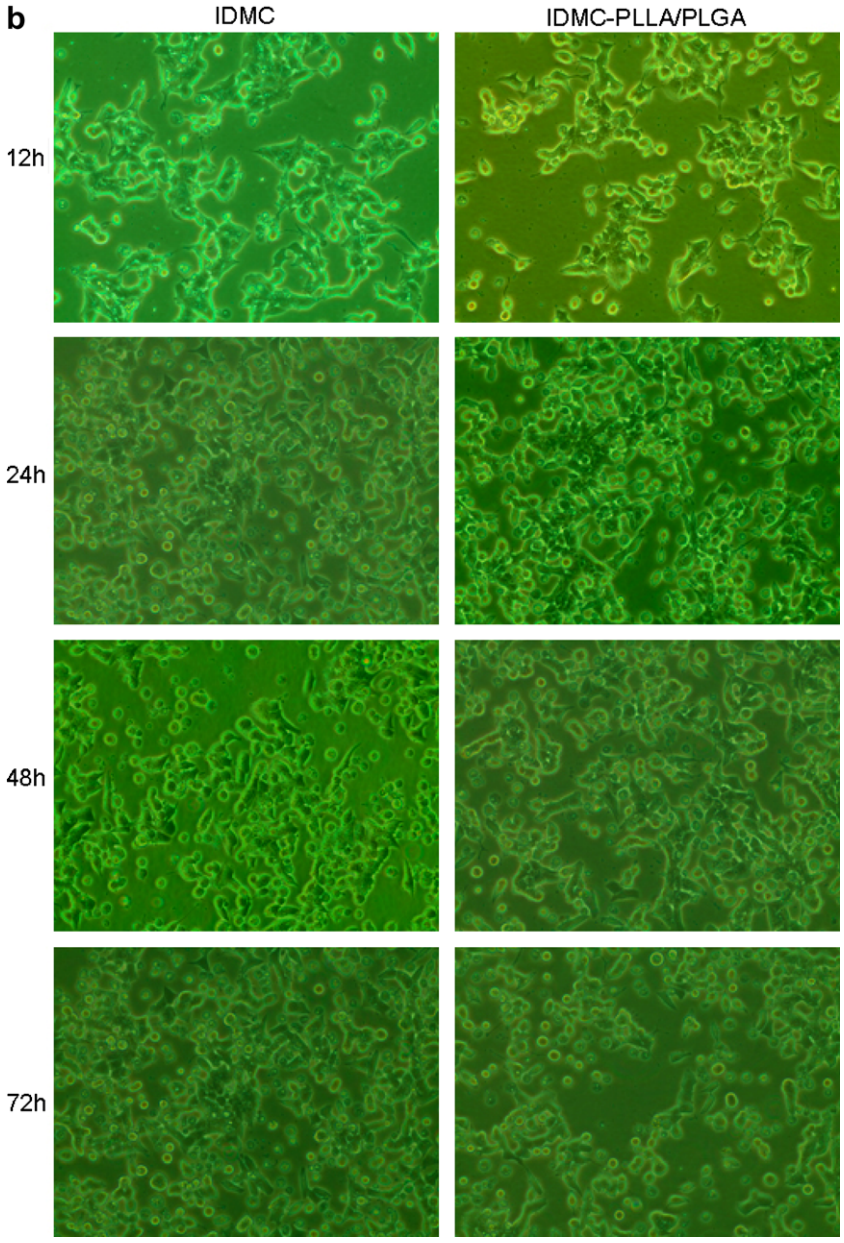

Fig 10. (*continued*)

In order to exclude possible cytotoxicity of carrier due to the change of particle size, carrier PLLA/PLGA was also evaluated *in vitro* by cytotoxicity tests, though the biocompatibility of PLLA and PLGA was authorized by FDA. The cell viability determined by MTT assay is normalized by the viability of cells cultured without microparticles, and thus, a value close to 100% is indicative of non-toxic cell culture conditions. To exclude the effects of sample pollution, the microparticles were sterilized by gamma-radiation for 72 h. Fig. 9 shows the cell viability of A549 cells incubated with the microparticles and free drug at 100 μM for designated time intervals (Fig. 9a), and at four different concentrations for 48 h (Fig. 9b). It is clearly indicated that placebo PLLA/PLGA microparticles have no effects on the cell proliferation of A549 cell. The optical images also show the good morphology of cell proliferation (Fig. 10a). This result is consistent with the good biocompatibility of PLLA and PLGA authorized by FDA. At the same time, this also indicates that the microparticles prepared by the SEDS process have little organic solvent residue. In our previous studies [19], the DCM residue in microparticles without any further treatment was 46 ppm, which was by far lower than the requirement of the *Pharmacopeia of the People's Republic of China* (2005) (max. 600 ppm) and was also lower than the one required by *the United States Pharmacopoeia* and *the European Pharmacopoeia* (400 and 600 ppm, respectively) [43].

It is observed from Fig. 9a that the cell viability of free IDMC is slower than that of IDMC-PLLA/PLGA microparticles containing IDMC at the same concentration of

IDMC before 48 h ($p < 0.05$). The free IDMC shows higher cytotoxicity than drug-loaded microparticles. After 48 h, the cell of free IDMC group begins to proliferate again, while the cell viability of IDMC-PLLA/PLGA microparticles group continues to decrease during the experimental period ($p < 0.05$). It is found from Fig. 10b that morphology of cells has significant differences between two groups after 48 h. The cells in free IDMC group begin to re-proliferate, the attachment of cells becomes well at 72 h. It could be inferred that free IDMC could begin to lose anti-cancer bioactivity after 48 h. While in IDMC-PLLA/PLGA microparticles group, the remains of dead cell can be found and the attachment ability of cell becomes poor. This could prove that the IDMC-loaded microparticles indicate sustained cell inhibition abilities against the A549 cell lines. This phenomenon appears to correspond reasonably well to the *in vitro* drug controlled release properties. From the *in vitro* drug release experiment, it is clearly shown that IDMC can gradually release from the microparticles and remain sustained release for 30 days, while the free IDMC reaches the concentration plateau in 48 h. The sustained cytotoxicity of drug-loaded microparticles may be related to the internalization of IDMC-loaded PLLA/PLGA microparticles into the cells and the successive drug release from microparticles inside the cells, enhancing the action of IDMC and preventing the inactivation of IDMC. In fact, the microparticles drug delivery system can act as a reservoir for IDMC, protecting the drug from hydrolysis and not only providing a sustained release of IDMC but also contributing to the maintenance of its activity.

Besides the incubation time, the microparticles concentration is also an important factor to determine the cytotoxicity. Fig. 9b shows the cytotoxicity of the free IDMC and microparticles with or without IDMC at 25, 50, 100 and 200 μM concentrations after 48 h at 37 °C. From the figure, it can be seen that the higher concentration leads to higher cytotoxicity. The IC_{50} of free IDMC and IDMC-PLLA/PLGA microparticles was 131.52±1.21 and 223.08±2.11 μM at 48 h exposure, respectively (Fig. 9b).

Therefore, it can be seen from Fig. 9 that the viability of non-small-cell lung cancer cell A549 decreases with increase of the drug concentration as well as the incubation time. The extended activity of IDMC from the drug-loaded microparticles might be explained by that microparticles can be adsorbed onto the cell membrane, generating a drug concentration gradient near the cell surface that could favor the drug to penetrate into the cell. Furthermore, the cell can phagocytize drug-loaded microparticles allowing the drug to be released inside the cytoplasm, thus contributing to a sustained drug concentration.

3.8. Fluorescence microscopy detection

Fluorescence microscopy may provide important information regarding interactions between drugs carriers and cells. Fig. 11 indicates the fluorescence photos of four groups. The cells without treatment (control group, Fig. 11a) show intact cell cytoskeleton and irregular nucleus. F-actins congregating silky arrangement and actin fibers aligned traversing the cytoplasm are observed in cells. For placebo microparticles group (Fig. 11b), the fluorescence morphology of cells is hardly altered, indicating no cytotoxicity of carriers PLLA/PLGA on cells. Further,

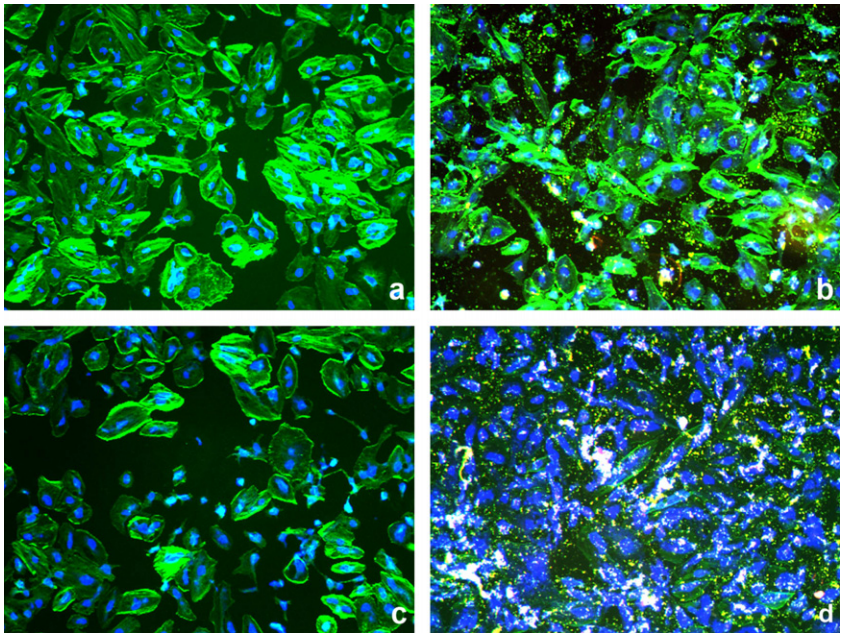

Fig. 11. Fluorescence microscopy of cell incubated after 24 h without microparticle (a), with fluorescent placebo microparticles (b), free IDMC solution (c), and fluorescent IDMC-loaded microparticles (d). Blue shows the cell nucleus, green shows cytoskeleton and yellow point (in b and d) indicates the fluorescent microparticles.

it can be observed that fluorescent microparticles (yellow point in the photo) are phagocytized into cells. For IDMC and IDMC-PLLA/PLGA groups (Fig. 11c and d), fluorescence photos of both cells demonstrate the classic nuclear morphologies such as chromatin margination, chromatin condensation, nuclear condensation, nuclear fragmentation. Disruption of the actin cytoskeleton is evidently associated with the regional distribution of F-actin cytoskeleton, showing a weak peripheral rim of the cytoplasm. Fig. 11d demonstrates that the A549 cells phagocytize the drug-loaded microparticles into the cytoplasm. These results suggest that IDMC-loaded microparticle was successfully phagocytized into the A549 cells and drugs released from carriers took effect of anti-tumor.

3.9. Cell ultrathin structure observation

To further understand the anti-tumor effects of drug-loaded microparticles, the ultrastructures of A549 cells cultured with placebo microparticles, IDMC-loaded microparticles, and free IDMC for 24 h were studied. The result of the TEM studies is shown in Fig. 12A–D. It is observed from TEM micrographs that A549 cells without any treatment indicate irregular nucleus, homogenously dispersed euchromatin and sunken nuclear membrane. Mitochondria, ribosome and rough endoplasmic reticulum (RER) can be all clearly observed in the cytoplasm. When the placebo microparticles were incubated with A549 cells, the phagocytosis of microparticles into the cytoplasm can be identified (Fig. 12B), while the ultrastructure of cells has no significant changes compared to the control group. This shows that the carriers have no cytotoxicity on cells, which is consistent with the results of MTT and fluorescence microscopy. It can be seen from Fig. 12C and D that free IDMC group and IDMC-loaded microparticles group both indicate that there are nuclear aberrations, mitochondria decrease and swelling, endoplasmic reticulum disintegration and lysosome increase of condensed cytoplasm.

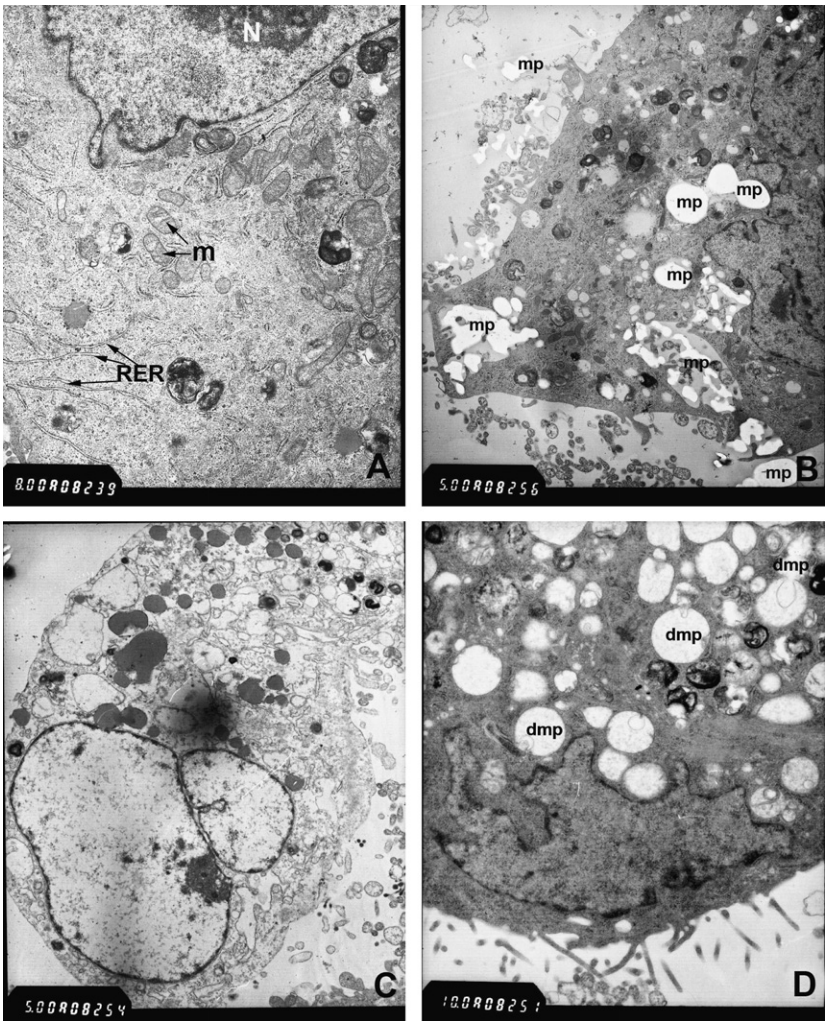

Fig. 12. Transmission electron microscopy of A549 cells: (A) without any treatments, 8000× magnification; N, nucleus; m, mitochondria; RER, rough endoplasmic reticulum; (B) placebo PLLA/PLGA microparticles, 5000× magnification; mp, microparticles; (C) free IDMC, 5000× magnification; (D) IDMC-loaded microparticles, 10,000× magnification; dmp, drugs-loaded microparticles. Cell apoptosis was observed through changes in the nucleus, euchromatin and mitochondria.

Margination and centralization of condensed chromatin also can be observed. This demonstrates that IDMC and drug-loaded microparticles both have the inhibition abilities of proliferation of A549 cancer cell at 24 h. An important aspect observed in this study is that IDMC-loaded microparticles can be successfully swallowed by cancer cell and the drugs can be gradually released from these microparticles, leading to cell apoptosis.

There are many evidences from epidemiological and laboratory studies, which had proved that IDMC has antitumor activity and reduces the incidence of colon cancer [44,45]. The use of IDMC-PLLA/PLGA delivery system in the treatment of A549 cell appears to be an attractive means of protecting the drug against fast inactivation (after 48 h). Those results in this study infer that IDMC-loaded PLLA/PLGA microparticles sustained delivery system has a new promising application in anti-cancer fields besides anti-inflammatory treatments, especially with the combination of other chemotherapy drugs [26]. These experimental results need to be further confirmed by *in vivo* experiments and clinical trials. In the next step, the *in vivo* study of IDMC-loaded PLLA/PLGA microparticles and new drug-loaded microparticles combined with other chemotherapy would be encouraged.

4. Conclusions

In this work, the SEDS process was successfully performed in the preparation of IDMC-PLLA/PLGA microparticles. The microparticles prepared in $scCO_2$ had smooth surface with small particle size and narrow particle size distribution. XRD, DSC results suggested that the drug was dispersed into the PLLA/PLGA polymer matrix in an amorphous form, which facilitated the diffusion and dissolution of IDMC in release medium. FTIR spectroscopy indicated a successful encapsulation of IDMC into PLLA/PLGA polymer matrix in the SEDS process. The drug release of IDMC-PLLA/PLGA microparticles was controlled by the diffusion of IDMC at the early stage and by the erosion of biodegradable polymer at the subsequent stage. The drug would release completely from drug-loaded PLLA/PLGA microparticles in a stable way. Cytotoxicity studies indicated that IDMC-loaded microparticles had sustained cell inhibition abilities against the proliferation of non-small-cell lung cancer A549 cell lines. Drugs-loaded microparticles can be phagocytized by A549 cells. After IDMC-PLLA/PLGA microparticles treatment, cell apoptosis was evidently observed from nuclear condensation, margination and centralization of chromatin, and mitochondria swelling and destruction. The great advantage of using IDMC-loaded microparticles is the fact that microparticles are located inside the cytoplasm and drugs can release gradually into the interior of cell, thus improving the therapeutic efficacy of IDMC and preventing the fast inactivation of free drugs. These results indicated IDMC-loaded microparticles as the formulation of solid dosage prepared by the SEDS process could be very promising drug delivery system for anti-cancer clinical applications. The results should be further confirmed by *in vivo* experiments.

Acknowledgements

Financial supports from the *Fund for Excellent Youth Teachers of Education Ministry of China* (2002123) and *Key Technologies Research and Development Program of Sichuan* (2006Z08-001-1) Province are gratefully acknowledged. We thank Wang Hui in the Analytical and Testing center of Sichuan University for performing SEM observation.

References

[1] C. Perez, I.J. Castellanos, H.R. Costantino, W. Al-Azzam, K. Griebenow, Recent trends in stabilizing protein structure upon encapsulation and release from bioerodible polymers, J. Pharm. Pharmacol. 54 (2002) 301–313.
[2] S.R. Bhatia, S.F. Khattak, S.C. Roberts, Polyelectrolytes for cell encapsulation, Curr. Opin. Colloid. Interface Sci. 10 (2005) 45–51.
[3] R. Langer, Drug delivery and targeting, Nature 392 (1998) 5–10.
[4] J.W. Tom, P.G. Debendetti, Formation of bioerodible polymeric microspheres and microparticles by rapid expansion of supercritical solution, Biotechnol. Prog. 7 (1991) 403–411.
[5] D.D. Hile, M.L. Amirpour, A. Akgerman, M.V. Pishko, Active growth factor delivery from poly(D,L-lactide-co-glycolide) foams prepared in supercritical CO_2, J. Control. Release 66 (2000) 77–185.
[6] M. Rodrigues, N. Peirico, H. Matos, E. Gomes de Azevedo, M.R. Lobato, A.J. Almeida, Microcomposites theophylline/hydrogenated palm oil from a PGSS process for controlled drug delivery systems, J. Supercrit. Fluids 29 (2004) 175–184.
[7] R.F. Falk, T.W. Randolph, Process variable implications for residual solvent removal and polymer morphology in the formation of gentamycin-loaded poly (L-lactide) microparticles, Pharm. Res. 15 (1998) 1233–1237.
[8] N. Foster, R. Mammucari, F. Deghani, Processing pharmaceutical compounds using dense gas technology, Ind. Eng. Chem. Res. 42 (2003) 6476–6493.
[9] S.G. Kazarian, Polymer processing with supercritical fluids, Polym. Sci. Ser. C 42 (2000) 78–101.
[10] M. Hanna, P. York, Patent WO 95/01221, 1994.
[11] M. Hanna, P. York, Patent WO 96/00610, 1995.
[12] J. Jung, M. Perrut, Particle design using supercritical fluids: literature and patent survey, J. Supercrit. Fluid 20 (2001) 179–219.
[13] S.D. Yeo, E. Kiran, Formation of polymer particles with supercritical fluids: a review, J. Supercrit. Fluid 34 (2005) 287–308.
[14] P. Chattopadhyay, R.B. Gupta, Production of antibiotic nanoparticles using supercritical CO_2 as antisolvent with enhanced mass transfer, Ind. Eng. Chem. Res. 40 (2001) 3530–3539.
[15] N. Elvassore, A. Bertucco, P. Caliceti, Production of protein-loaded polymeric microcapsules by compressed CO_2 in a mixed solvent, Ind. Eng. Chem. Res. 40 (2001) 795–800.
[16] M. Sarkari, J. Brown, X.X. Chen, S. Swinnea, R.O. Williams III, K.P. Johnston, Enhanced drug dissolution using evaporative precipitation into aqueous solution, Int. J. Pharm. 243 (2002) 17–31.
[17] T.L. Rogers, A.C. Nelsen, J.H. Hu, J.N. Brown, M. Sarkari, T.J. Young, et al., A novel particle engineering technology to enhance dissolution of poorly water soluble drugs: spray-freezing into liquid, Eur. J. Pharm. Biopharm. 54 (2002) 271–280.
[18] J.H. Hu, K.P. Johnston, R.O. Williams III, Spray freezing into liquid (SFL) particle engineering technology to enhance dissolution of

poorly water soluble drugs: organic solvent versus organic/aqueous co-solvent systems, Eur. J. Pharm. Sci. 20 (2003) 295–303.
[19] A.Z. Chen, X.M. Pu, Y.Q. Kang, L. Liao, Y.D. Yao, G.F. Yin, Preparation of 5-Fluorouracil-poly(L-lactide) microparticles using solution-enhanced dispersion by supercritical CO_2, Macromol. Rapid. Commun. 27 (2006) 1254–1259.
[20] K.S. Anil, W. Hardeep, Zinc–indomethacin complex: synthesis, physicochemical and biological evaluation in the rat, Int. J. Pharm. 120 (1995) 145–155.
[21] D. Chandrasekar, R. Sistla, F.J. Ahmad, R.K. Khar, P.V. Diwan, The development of folate-PAMAM dendrimer conjugates for targeted delivery of anti-arthritic drugs and their pharmacokinetics and biodistribution in arthritic rats, Biomaterials 28 (2007) 504–512.
[22] P.F. Coogan, L. Rosenberg, J.R. Palmer, B.L. Strom, A.G. Zauber, P.D. Stolley, S. Shapiro, Nonsteroidal anti-inflammatory drugs and risk of digestive cancers at sites other than the large bowel, Cancer Epidemiol. Biomark. Prev. 9 (2000) 119–123.
[23] A.L. Hsu, T.T. Ching, D.S. Wang, X. Song, V.M. Rangnekar, C.S. Chen, The cyclooxygenase-2 inhibitor celecoxib induces apoptosis by blocking Akt activation in human prostate cancer cells independently of Bcl-2, J. Biol. Chem. 275 (2000) 11397–11403.
[24] R.D. Maca, Enhancement of etoposide and methotrexate sensitivity by indomethacin in vitro, Anticancer Drug Des. 6 (1991) 453–466.
[25] C. Ruegg, J. Zaric, R. Stupp, Non steroidal anti-inflammatory drugs and COX-2 inhibitors as anti-cancer therapeutics: hypes, hopes and reality, Ann. Med. 35 (2003) 476–487.
[26] M.A. Hull, S.H. Gardner, G. Hawcroft, Activity of the non-steroidal anti-inflammatory drug indomethacin against colorectal cancer, Cancer Treat. Rev. 29 (2003) 309–320.
[27] L.J. Hixson, D.S. Alberts, M. Krutzsch, J. Einsphar, K. Brendel, P.H. Gross, et al., Antiproliferative effect of nonsteroidal antiinflammatory drugs against human colon cancer cells, Cancer Epidemiol. Biomarkers. Prev. 3 (1994) 433–438.
[28] P.G. Denbenedetti, J.W. Tom, S.D. Yeo, G.B. Lim, Application of supercritical fluids for the production of sustained delivery devices, J. Control. Release 24 (1993) 27–44.
[29] K.H. Song, C.H. Lee, J.S. Lim, Preparation of L-PLA submicron particles by a continuous supercritical antisolvent precipitation process, Korean J. Chem. Eng. 19 (2002) 139–145.
[30] T. Wu, Y. Sun, N. Li, M.M. de Villiers, L. Yu, Inhibiting surface crystallization of amorphous indomethacin by nanocoating, Langmuir 23 (2007) 5148–5153.
[31] G. Chandrashekar, N. Udupa, Biodegradable injectable implant systems for long term drug delivery using poly(lactic-co-glycolic) acid copolymers, J. Pharm. Pharmacol. 48 (1996) 669–674.
[32] C. Witschi, E. Doelker, Influence of the microencapsulation method and peptide loading on poly(lactic acid) and poly(lactic-co-glycolic acid) degradation during in vitro testing, J. Control. Release 51 (1998) 327–341.
[33] J.S.C. Loo, C.P. Ooi, F.Y.C. Boey, Degradation of poly(lactide-co-glycolide) (PLGA) and poly(L-lactide)(PLLA) by electron beam radiation, Biomaterials 26 (2005) 1359–1367.
[34] R. Ghaderi, P. Artursson, J. Carlfors, Preparation of biodegradable microparticles using solution-enhanced dispersion by supercritical fluids (SEDS), Pharm. Res. 16 (1999) 676–681.
[35] M.D. Blanco, R.L. Sastre, C. Teijón, R. Olmo, J.M. Teijón, Degradation behaviour of microspheres prepared by spray-drying poly(D,L-lactide) and poly(D,L-lactide-co-glycolide) polymers, Int. J. Pharm. 326 (2006) 139–147.
[36] L.G. Griffith, Polymeric biomaterials, Acta Mater. 48 (2000) 263–277.
[37] R. Liu, S.S. Huang, Y.H. Wan, G.H. Ma, Z.G. Su, Preparation of insulin-loaded PLA/PLGA microcapsules by a novel membrane emulsification method and its release in vitro, Colloid. Surface B 51 (2006) 30–38.
[38] R.P. Raffin, D.S. Jornada, M.I. Ré, A.R. Pohlmann, S.S. Guterres, Sodium pantoprazole-loaded enteric microparticles prepared by spray drying: effect of the scale of production and process validation, Int. J. Pharm. 324 (2006) 10–18.
[39] A.K. Singla, H. Wadhwa, Zinc-indomethacin complex: synthesis, physicochemical and biological evaluation in the rat, Int. J. Pharm. 120 (1995) 145–155.
[40] M. Timko, M. Koneracká, N. Tomašovičová, P. Kopčanský, V. Závišova, Magnetite polymer nanospheres loaded by Indomethacin for anti-inflammatory therapy, J. Magn. Magn. Mater. 300 (2006) e191–e194.
[41] D. Rusu, C. Cimpoiu, T. Hodisan, Control over a new preparation of indomethacin, J. Pharm. Biomed. Anal. 17 (1998) 409–413.
[42] H. Liu, N. Finn, M.Z. Yates, Encapsulation and sustained release of a model drug, indomethacin, using CO_2-based microencapsulation, Langmuir 21 (2005) 379–385.
[43] N. Elvassore, A. Bertucco, P. Caliceti, Production of insulin loaded poly(ethylene glycol)/poly (I-lactide) (PEG/PLA)nanoparticles by gas antisolvent techniques, J. Pharm. Sci. 90 (2001) 1628–1636.
[44] S. Sato, Y. Kwon, S. Kamisuki, N. Srivastava, Q. Mao, Y. Kawazoe, M. Uesugi, Polyproline-rod approach to isolating protein targets of bioactive small molecules: isolation of a new target of indomethacin, J. Am. Chem. Soc. 129 (2007) 873–880.
[45] A. Bernardi, M.C. Jacques-Silva, A. Delgado-Cañedo, G. Lenz, A.M.O. Battastini, Nonsteroidal anti-inflammatory drugs inhibit the growth of C6 and U138-MG glioma cell lines, Eur. J. Pharmacol. 532 (2006) 214–222.